Environ. Sci. Technol. **2002**, *36,* 2670−2676

Cesium Adsorption on Clay Minerals: An EXAFS Spectroscopic Investigation

BENJAMIN C. BOSTICK,[†] MURTHY A. VAIRAVAMURTHY,*[,‡] K. G. KARTHIKEYAN,[§] AND JON CHOROVER[⊥]

Stanford University, Department of Geological and Environmental Sciences, Stanford, California 94305-2115, Brookhaven National Laboratory, Energy Sciences and Technology Department, Upton, New York 11973, University of Wisconsin, Biological Systems Engineering Department, Madison, Wisconsin 53705, and University of Arizona, Department of Soil, Water and Environmental Sciences, Tucson, Arizona 85721-0038

Cesium adsorption on the clay minerals vermiculite and montmorillonite is described as a function of surface coverage using extended X-ray adsorption fine structure spectroscopy (EXAFS). Cesium (Cs) possessed a variable coordination environment consisting of Cs−O distances between 3.2 and 4.3 Å; however, disorder typical of the Cs coordination environments prevented the resolution of all oxygen shells. On the basis of the influence of Cs loading and exchangeability on this structural arrangement, we could recognize both inner-sphere and outer-sphere adsorption complexes. The shorter Cs−O bond distance belongs to outer-sphere complexes typical of hydrated ions. In inner-sphere complexes, partially or fully dehydrated Cs coordinates directly to siloxane groups of the clay minerals forming longer Cs−O bonds. The inner-sphere adsorption complexes may have occurred within the interlayer or at frayed edge sites and were less extractable than the outer-sphere complexed Cs. Both coordination number ratios and linear combination fitting of EXAFS spectra were useful in estimating the fractions of inner-sphere and outer-sphere adsorption complexes. Our results show that X-ray absorption spectroscopy (XAS), and particularly EXAFS, is a valuable technique for exploring the type of Cs binding in environmental samples.

Introduction

Soils and sediments contaminated by radionuclides and toxic metals pose serious environmental threats and challenge remediation. Contamination by highly soluble radionuclides, such as ^{137}Cs, is particularly dangerous because of their ability to move with aqueous media in the subsurface. In fact, large volumes of contaminated wastes containing these radionuclides have leaked from storage tanks or other sources at DOE sites, such as the Hanford and the Savannah River sites, and thence into nearby groundwater and canals (*1*−*3*). The mobility of these soluble radionuclides is controlled by their sorption onto soil particles (*4*−*6*). A variety of factors, including the solution pH, ionic strength, moisture content, competitive sorption, and complexation with inorganic and organic ligands, influence the type and extent of sorption, thereby affecting the environmental transport of these cations.

The Cs^+ ion does not form strong complexes with dissolved inorganic or organic ligands (e.g., EDTA), so that the sorption of the free ion on minerals is the dominant factor controlling its speciation and environmental fate. The major sorbents in soils are generally thought to be the layer-type silicates that bind Cs either through weak electrostatic interactions or through stronger bonds formed by partial sharing of electrons between Cs and the ligand sites of the clay mineral. Electrostatic associations of hydrated Cs with anionic surfaces within the basal plane or interlayer and dissociated edge hydroxyl groups form outer-sphere (OS) complexes. On the other hand, electronic bonding at the frayed edge sites (FES), external basal sites, or within the interlayer (*4*, *7*−*9*) generates inner-sphere (IS) complexes. The FES represent particularly high-affinity sorption sites in which Cs may coordinate directly to basal oxygens on adjacent siloxane groups. Because the radius of the dehydrated Cs^+ ion is similar to that of the ditrigonal siloxane cavity of layer silicates, adsorption of Cs^+ to negatively charged siloxane sites can result in inner-sphere complexation (*4*, *5*). The reactivity of the inner-sphere complexation sites may differ widely. The most reactive of these sites probably constitute only a small portion ($\sim 10^{-8}$ mol/kg) of the total (*3*, *7*, *10*). However, other relatively strong complexes may form at other surface sites at higher concentrations.

Isomorphic substitution of Al^{3+} for Si^{4+} in the tetrahedral sheet comprising the siloxane site (e.g., as with illite and vermiculite) enhances the stability of the Cs^+−siloxane surface complex, presumably by promoting the dehydration of the sorbed Cs cation (*4*, *11*). In contrast, when isomorphic substitution is restricted dominantly to the more distant octahedral sheet (e.g., as with montmorillonite), a weaker OS complex may result (*12*). Therefore, cesium adsorption and its subsequent transport are influenced by mineralogical differences and the associated crystal chemistry of clays. In Hanford-site soils, the dominant 2:1 layer silicate at shallow depths is montmorillonite (*13*), whereas illite and vermiculite are more prevalent in the surface layers (*2*, *3*, *14)*; thus, changes in sorption with depth may potentially influence Cs mobility along the flow path. Using ^{133}Cs magic angle spinning nuclear magnetic resonance (MAS NMR) spectroscopy, Kim and co-workers (*5*, *11*, *15*) and Brouwer et al. (*10*) found that much of the Cs sorbed to montmorillonite was present at interlayer sites. For illite, both the FES and crystallite basal surfaces participated in the sorption reaction (*13*, *16*). In fact, Brouwer et al. (*10*) identified multiple FES sites.

X-ray absorption spectroscopy (XAS), including both X-ray absorption near-edge structure (XANES) and extended X-ray absorption fine structure (EXAFS), is a nondestructive, element-specific technique to probe adsorbate structures at the mineral−water interface. Information from EXAFS, especially the number and distance of the nearest neighbors in the first and second shells, can be used to discern the predominant sorption mechanisms for concentrations as low as 50−100 mg/kg. For example, O'day et al. (*17*, *18*) identified different Co^{2+} sorption complexes (including mononuclear and multinuclear complexes) on kaolinite and Al_2O_3 surfaces as a function of adsorbate-to-adsorbent ratios. Such a knowledge is important because the type of sorption complex

* Corresponding author phone: (631) 344-5337; fax: (631) 344-7905; e-mail: vmurthy@bnl.gov.
[†] Stanford University.
[‡] Brookhaven National Laboratory.
[§] University of Wisconsin.
[⊥] University of Arizona.

10.1021/es0156892 CCC: $22.00
Published on Web 05/17/2002

dictates the trace element's solubility and, hence, the concentration available for transport. Outer-sphere adsorption complexes also were identified by XAS for Sr^{2+} adsorbed to iron oxides (*19*). EXAFS was used extensively to study other adsorption reactions, including Cr on magnetite (*20*, *21*), Cr on iron and manganese oxides (*22*), and Cr on silica (*23*, *24*). Recently, EXAFS was extended to probe the coordination of Cs to clay minerals (*25*) and crown ethers (*26*, *27*) at moderate concentrations of Cs. Generally, EXAFS and NMR are not sensitive enough to study systems where Cs is sorbed solely to the strongest binding sites because such sites constitute only a small fraction of the total amount of sorbed Cs (*3*, *7*, *10)*, probably amounting to levels below the detection limits of these techniques (*3*, *7*). Nevertheless, EXAFS may be useful to elucidate changes in the mechanism of Cs-binding over a significant range in surface coverage.

In this research, we employed EXAFS to determine the structure of Cs adsorbed to two clay minerals, montmorillonite and vermiculite, as a function of surface coverage. Montmorillonite's charge derives largely from the isomorphic substitution of Mg^{2+} for Al^{3+} in the octahedral sheet, whereas vermiculite's charge results from substituting Al^{3+} for Si^{4+} substitution in the tetrahedral sheet. Our EXAFS investigations of Cs coordination on these clays revealed different types of adsorption complexes, particularly as a function of surface coverage. The experiments also included EXAFS investigations of illite, which occur in the region of leaking tanks at the Hanford site. However, the data could not be refined successfully because of poor spectral quality.

Materials and Methods

Pretreatment and Cs Saturation of Clay Minerals. Specimens of the clay minerals Wyoming montmorillonite (SWy-2) and Silver Hill illite (IMt-1) were acquired from the Source Clay Minerals Repository, University of Missouri, and vermiculite was purchased from Ward's Natural Science Establishment, Inc., NY. For montmorillonite, 200 g of the untreated clay were added to 1 kg of ultrapure (MilliQ) water and dispersed for size fractionation, adjusting the pH of the suspension to 8.0 by adding small aliquots of 0.01 M NaOH while mixing for 45 min with a magnetic stirrer. The $<2\ \mu$m size fraction was isolated by repeated dispersion and centrifugation of the original material (5 min at 1000 rpm, 25 °C). The clay suspension then was flocculated by adding 0.001 M HCl in 1.0 M NaCl and mixing for 20 min. To remove oxide impurities, the clays were dispersed and washed repeatedly, each time for 20 min, in 1.0 M NaCl preadjusted to pH 3 (0.001 M HCl) until the pH value of the supernatant solution reached pH 3. The clays were redispersed in 0.01 M NaCl solution and the washing procedure repeated (without HCl) until the pH of the supernatant solution reached 5.5. The concentration of clay was adjusted to give a solid concentration in stock suspension of 200 g/kg. The illite and vermiculite clays were pretreated and purified as detailed in Sposito and LeVesque (*28*). The $<106\ \mu$m (effective diameter) size fractions were obtained by sedimentation and centrifugation. All clays were stored as stock aqueous suspensions before use.

The clay minerals were saturated with Cs by equilibrating a clay mineral suspension (1:25 solid/solution ratio) once with 0.5 M CsCl (for 1 h), twice with 0.1 M CsCl (1 h), and once with 0.05 M CsCl (8 days). This approach was shown to completely saturate Cs-accessible adsorption sites (*29*). The Cs content of the saturated clays was determined by combining the Cs extracted from two NaCl exchange steps followed by two extractions with 1 M ammonium acetate at pH 7. To obtain samples with a range of Cs surface coverage for EXAFS analysis, the Cs-saturated clays were exchanged twice (for 30 min each time) with 0.01 M NaCl to displace Cs^+ from sites with lower Na^+ to Cs^+ selectivity. The surface Cs concentrations following exchange steps were determined by measuring the Cs released into solution by atomic emission spectrometry and sorbed Cs was calculated by difference. Entrained Cs was removed by ethanol washing steps, so the EXAFS signal is limited to sorbed Cs. Spectra were collected on Cs-saturated clays, as well as samples subjected to one and two Na^+ exchange steps.

We also examined the spectra of Cs-substituted clinoptilolite (a common natural zeolite) because it is one of the few Cs-containing solid phases for which information is available on Cs coordination environment and for which there is a good crystal structure (*30*). The reference clinoptilolite from Castle Creek, ID, that we used was obtained from Minerals Research Inc., Clarkson, NY. Repeated washings with dilute HCl and water purified the sample before saturated with Cs, as described in earlier sections.

XAS Spectroscopy. X-ray absorption spectra of Cs-sorbed clay minerals were collected as fluorescence excitation spectra using a passivated implanted planer silicon (PIPS) detector (Canberra Industries, CT) at the National Synchrotron Light Source (NSLS) X-19A beam line at the Brookhaven National Laboratory. The storage ring operated at 2.8 GeV and at currents of approximately 250 mA. In the X-19A beam line, the X-ray beam was diffracted by a double-crystal Si(111) monochromator which passes a narrow energy band to the sample. The monochromator was detuned by ca. 70% to minimize higher-order harmonics in the X-ray beam. X-ray absorption spectra were collected from −200 to +700 eV about the L_{III}-edge of Cs (5012 eV). External energy calibration was achieved by running initial spectra of CsCl and setting the inflection point of CsCl at 5015 eV; this calibration drifted less than 0.5 eV during the experiments. For X-ray analysis, samples were sealed in a X-ray film bag (2.5 μm Prolene or Mylar from Chemplex Industries, NY) and attached to the sample holder at the beam line.

The EXAFS spectra were analyzed using WinXAS (*31*). Following spectral averaging, the background was subtracted from the spectra using a polynomial fit and normalizing the resulting heights of the spectral jump to unity. A seven-point cubic spline function that followed the envelope of the decaying spectrum was used to isolate the EXAFS spectral contribution (the $\chi(k)$ function). The energy (eV) scale was transformed to momentum space (k-space, units of $Å^{-1}$) using 5020 eV as the energy of the Cs L_{III} edge (E_0). The $\chi(k)$ spectrum then was weighted by k^3 to amplify the upper k-range and Fourier-transformed without smoothing to produce a radial structure function (RSF) using a k-range of approximately 1.8−7 $Å^{-1}$. This limited k-range was adequate to fit five variables. Distinct shells of the RSF were then back-transformed to isolate the spectral contributions of each atomic shell. Final fits were completed using unfiltered k-weighted $\chi(k)$ spectra.

The type (Z), coordination number (CN), interatomic distance (R), and the Debye−Waller factor (σ^2) of the atoms coordinating Cs were determined by fitting the experimental spectrum using phase and amplitude functions derived with FEFF 7.02 (*32*, *33*). The Debye−Waller factor is effectively the variance in bond length and is a measure of the disorder of the coordination environment. Two Cs−O shells were used in fitting; the CN and R were varied for each shell, while E_0 and σ^2 were constrained to minimize the number of variables. E_0 was constrained to the same value for each shell. The fitting of Fourier-filtered shells consistently yielded σ^2 values between 0.01 and 0.02; therefore, σ^2 was constrained at 0.015. The third cumulant fit parameter was also used to account for the anisotropy caused by the large degree of disorder present in the local structure of Cs. The third cumulant was fixed at 0.0025 for all shells because this value was consistent with reference spectra and yielded reasonable coordination numbers. Once the filtered spectra were fit, the resulting

TABLE 1. Cesium Adsorption to Montmorillonite, Illite, and Vermiculite after Cs Saturation and Following Successive Extractions with 0.01 M NaCl

clay mineral	sorption capacity (mmol/kg)	q_{Cs} (mmol/kg)		K_d[b] (mL/g)		K_c[c]	
		wash 1	wash 2	wash 1	wash 2	wash 1	wash 2
montmorillonite	783 ± 0.6[a]	626 ± 5.2	538 ± 7.2	399	611	21.4	63.4
vermiculite	271 ± 6.8	191 ± 2.0	159 ± 1.5	239	497	27.5	150.3
illite	150 ± 2.9	90 ± 2.2	68 ± 0.7	150	309	23.5	137.4

[a] Values are the average of three replicates ± the standard deviation. [b] K_d, the distribution coefficient, is defined as the ratio of adsorbed to dissolved Cs concentrations. [c] K_c, the selectivity coefficient, is defined by the relationship $K_c = ([Na^+]\{Cs - X\})/([Cs^+]\{Na - X\})$, where brackets denote soluble ion concentrations and braces describe adsorbed concentrations of Cs^+ and Na^+ on site X.

parameters were combined and refit to the unfiltered $\chi(k)$ spectrum. The accuracy of the fits was estimated using the χ^2 statistical parameter, for which smaller values correspond to the best fits. By comparison with model compounds, the interatomic distances can be determined within 0.09 Å and the coordination number within 30% for the first shell, though less accurately for more distant shells.

Results and Discussion

Cesium adsorption capacity was largest for montmorillonite and decreased significantly for vermiculite and illite (Table 1). The higher sorption to montmorillonite probably reflects the increased availability of interlayer sorption sites on the expansible montmorillonite clay. Washing with 0.01 M NaCl resulted in the exchange of Cs^+ for Na^+ on the clays, displacing a large fraction of Cs from each clay mineral. Because Na^+ is a strongly hydrated cation that forms OS surface complexes, Na^+-Cs^+ exchange is presumed to be very effective in removing weakly bound Cs species. Nearly 245 mmol/kg (about 31% of the total) of the adsorbed Cs on montmorillonite was removed in two exchange steps. Lower total amounts of Cs were removed by sodium exchange on illite and vermiculite (about 82 and 112 mmol of Cs/kg, respectively), but they represented a higher fraction of the initial sorbed amount such that the relative losses were higher (54% and 41% of the total, respectively).

The first Na^+ exchange step removed a larger fraction of adsorbed Cs than the second one, particularly for Cs-sorbed illite and vermiculite. These extractions are best explained by examining the changes in partition coefficient (K_d) and the selectivity coefficient (K_c). A constant value of K_d and K_c would suggest that only one type of adsorption complex is present, while variation with coverage is consistent with Cs^+ retention in multiple types of coordinative environments. Both K_d and K_c increase with decreasing Cs^+ loading, suggesting that multiple types of adsorption complexes are formed. The trend in increasing K_d and K_c with repeated Na^+ exchange is consistent with the preferential displacement of weakly bound species (presumably OS) and retention of a higher fraction of more stable surface complexes (*3*, *6*). Because weakly held species are displaced, residual species are bound more tightly overall. Therefore, both IS and OS complexes are likely present in these samples. Furthermore, the largest values of K_c, indicative of the greatest selectivity and thus the largest fraction of IS complexes, are found for illite and vermiculite that contain the largest fraction of high-affinity, frayed-edge sites (*4*, *5*, *7*, *8*, *10*). Inner-sphere complexes also may form in the interlayer adjacent to locations where isomorphous substitution occurs in the tetrahedral sheet. In such environments, Cs coordination to the ditrigonal cavity within the tetrahedral sheet of vermiculite and illite causes partial collapse of the interlayer (*34*, *35*), rendering the interlayer Cs less exchangeable than Cs adsorbed to planar sites (*36*, *37*) (Figure 1).

Although the Cs^+-Na^+ exchange data suggest that multiple adsorbed Cs species are present on these clay minerals, additional information is needed from Cs EXAFS

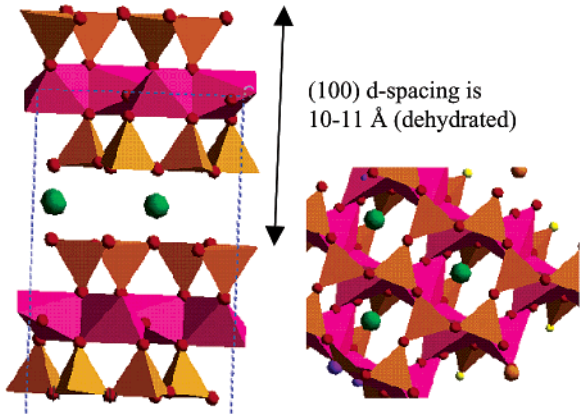

FIGURE 1. Model structure for Cs-sorbed clays, showing the formation of an inner-sphere complex for the Cs atom (green) within the trigonal layer of the phyllosilicate interlayer. The (001) *d* spacing is about 12−14 Å for partially hydrated, Cs-exchanged, 2:1 clay minerals; the *d* spacing decreases to 10 Å when fully dehydrated (as shown).

to characterize them adequately. Unfortunately, the presence of multiple coordination environments complicates quantitative analysis of such, often preventing successful analysis and interpretation (*21*). The presence of static disorder in the local structure of Cs is a further hindrance. To gain more insight into the effects of this disorder on the EXAFS spectra, we used the spectra Cs-substituted clinoptilolite for which information is available on Cs coordination environment (*30*). Table 2 gives the interatomic distances of Cs-substituted clinoptilolite and illustrates this disorder. The Cs−O distances are between 3.2 and about 4 Å in the first coordination sphere. The variation in the lengths of the Cs−O bonds has important consequences for EXAFS fitting. First, spectral intensity is decreased due to phase cancellation, lowering the apparent coordination number for a given shell. More importantly, EXAFS spectroscopy is more sensitive to atoms at shorter distances. Therefore, much of the spectral intensity of a highly disordered shell originates from the nearest atoms in the shell, generating a fit distance that is shorter than the actual average distance. The third cumulant partially corrects for this asymmetry and is essential for accurately analyzing Cs coordination environments. Table 3 shows our fits of EXAFS data of a similar Cs-saturated clinoptilolite. Even with this correction, the calculated interatomic distances of Cs-saturated clinoptilolite are significantly contracted due to static disorder and the coordination numbers are reduced relative to their actual values (Table 2). These problems are less significant for Cs in confined coordination environments, such as crown ethers (Table 3). In such systems, Cs−O bond lengths are more regular, and consequently, they are the only examples of Cs-coordination environments quantified using EXAFS.

The Cs EXAFS spectra of Cs-saturated vermiculite and montmorillonite contain two principal coordination shells (Figures 2 and 3). Although spectra for Cs-loaded illite samples

TABLE 2. Cesium Coordination Environments for Selected Species[a]

sample	bond	CN	R (Å)	R_{ave} (Å)	σ^2 (Å^2)	ref
Cs−clinoptilolite	Cs−O	2	3.21	3.50	0.06	*30*[b]
	Cs−O	1	3.38			
	Cs−O	2	3.42			
	Cs−O	2	3.78			
	Cs−O	1	3.80			
	Cs−O	1	4.14	4.55	0.047	
	Cs−O	3	4.42			
	Cs−O	2	4.56			
	Cs−O	2	4.67			
	Cs−O	2	4.81			
	Cs−Si/Al	2, 2, 4	4.00, 4.12, 4.45	4.25	0.045	
Cs chelated by 18-crown-6	Cs−O	6	3.23			*27*[c]
Cs chelated with dibenzo-18-crown-6 bromide	Cs−O	6	3.04			*25*[c]
	Cs−Br	1	3.60			

[a] The average interatomic distance (R_{ave}) and its variance (σ^2) illustrate the static disorder present in these systems. Other Cs-containing phases have similar disorder in the Cs−O coordination spheres. The interatomic distances of Cs-saturated clinoptilolite were determined by XRD and are included for comparison to the coordination environment determined in our study by XAS (Table 3). [b] Determined using diffraction methods. [c] Determined using XAS.

TABLE 3. Cesium Local Structure Determined Using EXAFS Data for Cs-Sorbed Clays and for Cs−Clinoptilolite[a]

sample	coverage (mmol/kg)	bond	CN	R (Å)	σ^2 (Å^2)[b]	N_s/N_l[e]
Cs on montmorillonite	783	Cs−O_s[c]	2.25	3.08	0.015	0.32
		Cs−O_l[d]	7.00	4.17	0.015	
Cs on montmorillonite	627	Cs−O_s[c]	2.84	3.22	0.015	0.27
		Cs−O_l[d]	10.53	4.27	0.015	
Cs on montmorillonite	538	Cs−O_s[c]	3.28	3.29	0.015	0.24
		Cs−O_l[d]	13.08	4.35	0.015	
Cs on vermiculite	271	Cs−O_s[c]	2.30	3.23	0.015	0.24
		Cs−O_l[d]	9.82	4.29	0.015	
Cs on vermiculite	190	Cs−O_s[c]	2.02	3.22	0.015	0.22
		Cs−O_l[d]	9.67	4.29	0.015	
Cs on vermiculite	159	Cs−O_s[c]	2.15	3.22	0.015	0.20
		Cs−O_l[d]	10.73	4.29	0.015	
Cs−clinoptilolite		Cs−O_s[c]	4.15	3.22	0.015	1.11
		Cs−O_l[d]	3.73	4.29	0.015	

[a] The coordination number is typically accurate to within 30%, the interatomic distance R within 0.09 Å, and the Debye−Waller factor (σ^2) represents the variance in R. The third cumulant was fixed at 0.0025 for all shells to minimize the number of floating parameters and allow for uniform data analysis. For all of the media, E_0 was at near +3 eV, about 5015 eV. [b] These parameters were fixed during fitting. [c] Short Cs−O distance, assigned to OS complexes. [d] Long Cs−O distance, assigned to IS complexes. [e] Ratio of hydrated (OS) to dehydrated (IS) Cs−O coordination numbers.

were also obtained, the lower solid-phase concentration of Cs (Table 1) and spectral interference near the Cs L_{III}-edge prevented refinement of the data. The first shell, at an uncorrected distance of about 2.7 Å, represents the shortest Cs−O bonds. The second Cs−O shell, found for more distant oxygen atoms, is at an uncorrected distance of 3.9 Å. The first peak is fit with a Cs−O shell at a distance of 3.2 Å, while the latter peak is fit with a larger Cs−O shell at 4.25 Å (Table 3). Aluminum or Si shells also would result from IS Cs coordination; however, no Cs−Al or Cs−Si shells were required to fit the data. Although such IS complexes are likely to be present, their weak scattering efficiency at longer radial distances prevents their detection. Despite this limitation, the IS and OS coordination environments can be differentiated by carfeully analyzing the two Cs−O shells.

To interpret these spectra, we needed to establish a model of adsorption that is consistent with both Na^+ exchange data and other sources. The exchange data and prior studies (*4*, *5*, *7*, *8*, *10*) consistently suggest the presence of two principal surface species, broadly defined here as inner- and outer-sphere complexes. These complexes are distinguished by distinct Cs−O coordination environments. In outer-sphere complexes, the Cs ion adsorbs with its hydration shell intact; thus, the Cs−O bond distances will be comparable to those for Cs ions in aqueous solution. Hydrated cesium ions exhibit a lower coordination number than other Cs ions (including inner-sphere ions), thereby reducing the Cs−O distance (*38*). Consequently, the Cs−O bond distances in hydrated Cs are about 3.0−3.2 Å. In contrast, the Cs−O distances are longer in inner-sphere complexes that form through partial dehydration and the formation of a Cs-surface chemical bond. For example, Cs-exchanged clinoptilolite and Cs-muscovite, which are dehydrated IS complexes similar to those likely occurring on clay minerals, have Cs−O distances between 3.34 and 4.8 Å, calculated using the crystallographic parameters published previously (*30*, *39*). As shown in Table 2 for Cs-exchanged clinoptilolite, this large spread in the Cs−O distance stems from the presence of disordered first- and second-shell oxygens.

The significant difference in Cs−O coordination parameters between inner-sphere and hydrated Cs provides a basis for identifying them. The majority of the 3.2 Å Cs−O shell arises from OS Cs sorption, while the more distant Cs−O peak represents IS complexes. However, this distinction is not absolute because both IS and OS complexes possess a range of Cs−O distances and thus have spectral contributions that arise from both 3.2 and 4.0+ Å shells. For example, Cs-exchanged clinoptilolite has two Cs−O shells fit with a roughly equal coordination number (Table 3). However, the samples with the largest coordination numbers in the first shell will

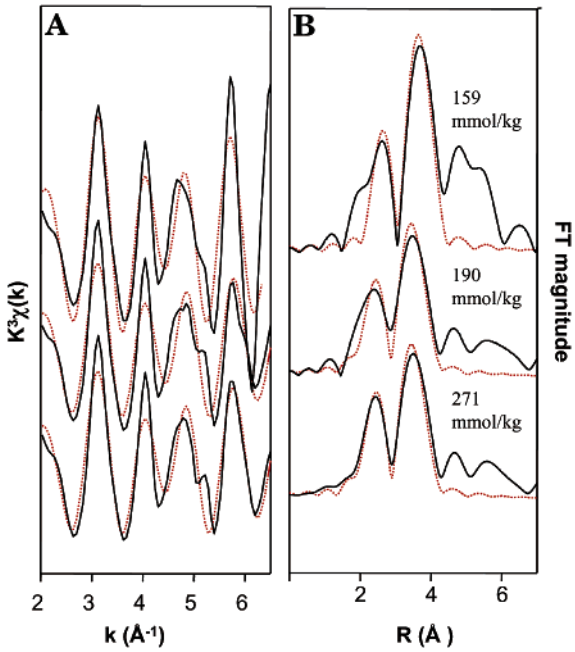

FIGURE 2. (A) k^3-weighted $\chi(k)$ Cs-L_{III} EXAFS spectra and (B) their uncorrected radial structure functions for Cs-sorbed vermiculite as a function of Cs loading. The experimental data (solids lines) are fit (dotted lines) using the parameters described in Table 3.

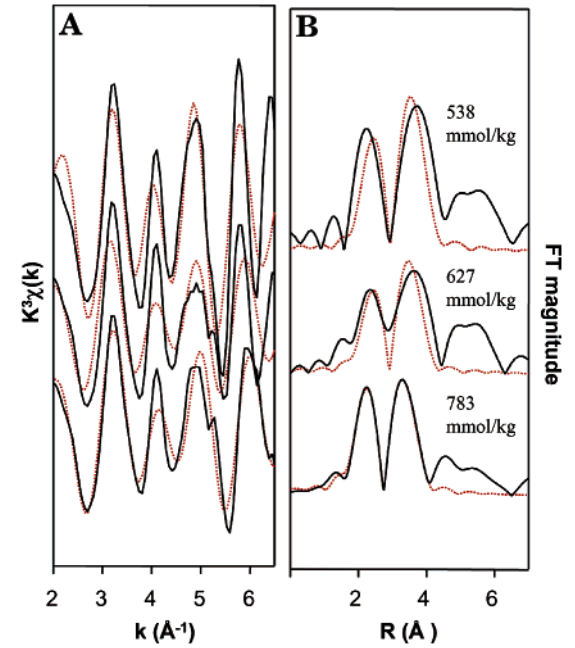

FIGURE 3. (A) k^3-weighted $\chi(k)$ Cs-L_{III} EXAFS spectra and (B) their uncorrected radial structure functions for Cs-sorbed montmorillonite as a function of Cs loading. The experimental data (solids lines) are fit (dotted lines) using the parameters described in Table 3.

be those with the shortest bond lengths and, therefore, dominantly OS coordination. The ratio of coordination numbers for each Cs−O shell (~3.2 to ~4.2 Å Cs−O) serves to quantify the transition between surface species; it should be largest for samples in which Cs adsorption is predominantly OS and decrease with increasing fraction of IS complexes. This ratio is more sensitive to relative changes in coordination between sites than to changes in coordination number alone. Thus, the CN ratio provides a qualitative measure of relative IS and OS site populations for a particular substrate.

The assignment of OS and IS complexes to short and long Cs−O bonds, respectively, is supported by the effect of surface coverage on the spectra. For Cs sorbed on vermiculite, the relative Fourier transform (FT) magnitude of the first Cs−O peak compared to the second one is highest for Cs saturated samples and decreases progressively with Na^+ exchange (Figure 2). (FT magnitude is proportional to the coordination number.) Similar trends are observed for Cs sorbed on montmorillonite (Figure 3) and are accompanied by the elongation of the OS bond. This progression toward a smaller CN for the short Cs−O bond distance with increased ion exchange is consistent with assigning of this spectral feature to OS sorption complexes. Following Cs sorption, both IS and OS surface complexes are present. Exposing the samples to NaCl solution preferentially removes the labile outer-sphere Cs, so that a higher fraction of adsorbed Cs remains on IS sites. The ratio of OS to IS coordination numbers (Table 3) quantitatively describes the shift in coordination toward longer Cs−O distances that are indicative of IS complexes. For montmorillonite, the CN ratio decreases from 0.32 for the 783 mmol/kg sample to 0.24 for the 538 mmol/kg sample. The peak ratio for vermiculite decreases as well, from 0.24 to 0.20 with decreasing surface coverage. Although the relative change in peak ratios is small, the spectral changes observed support a two-site model of Cs adsorption.

Comparison between the different clay minerals also sustains our designation of the 3.2 Å Cs−O distance to outer-sphere adsorption complexes. Montmorillonite saturated with Cs contains the largest OS/IS coordination number ratio, consistent with the hypothesis that it has the largest fraction of OS Cs species. In contrast, the vermiculite spectra change much less because a larger fraction of the sorbed Cs forms inner-sphere complexes in association with charged tetrahedral sites. Thus, both IS and OS surface complexes can be identified from fitting the EXAFS data.

Linear combination fitting of EXAFS data offers an alternative method of quantifying IS and OS complexes on clay minerals. Such methods eliminate the dependence on small changes in relative coordination number. In fact, they do not depend on EXAFS fitting at all, which only is approximate for such disordered systems. Instead, they depend on a linear combination of end members with known compositions and structures. For our two-site model of Cs adsorption, IS and OS reference spectra must serve as these end members. Unfortunately, pure IS and OS Cs reference spectra are not available but they can be approximated based on our understanding of the local chemical environments. The sample of montmorillonite with the highest coverage (783 mmol/kg) may be defined as being dominated by OS complexes, whereas the vermiculite sample with the lowest coverage (159 mmol/kg) likely has the largest fraction of IS complexes. Therefore, these two samples can serve as OS and IS references, respectively, because we can describe the other spectra as linear combinations of them. This quantification method does not distinguish between multiple IS complexes, although probably they are present. However, many of these IS complexes are found only in small relative concentrations (*3*, *7*, *11*) and are probably not detected by bulk EXAFS analysis. While these end members certainly are not pure standards, their combination may be used to quantify changes in Cs coordination with Na^+ exchange.

A significant change in the fraction of IS and OS complexation was apparent using linear combination fitting of the spectra (Figure 4). For montmorillonite, the fraction of OS complex (defined arbitrarily as 783 mmol/kg on montmorillonite) decreased from 100% to 52% with washing (Table 4). Although it is unlikely that all Cs sorbed to Cs-saturated montmorillonite was OS, IS complexes are not resolvable since the whole spectrum was used as a reference in fitting. Cs-sorbed vermiculite exhibited similar trends. The decrease

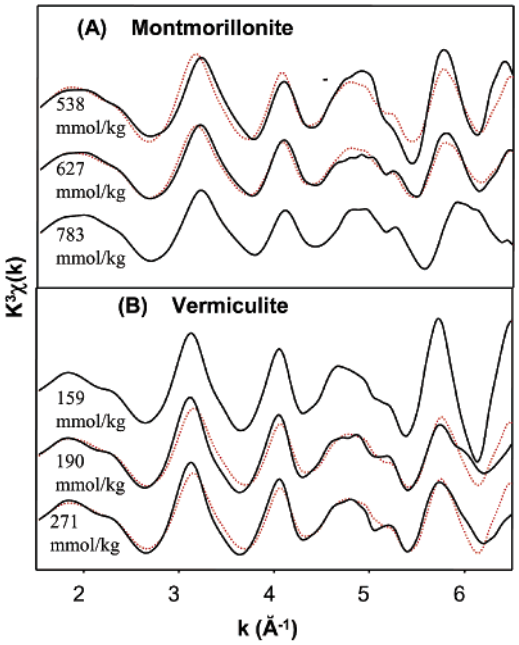

FIGURE 4. Linear combination fitting of the k^3-weighted $\chi(k)$ Cs-L_{III} EXAFS spectra for Cs-sorbed montmorillonite (A) and vermiculite (B) assuming two samples as end members for IS (159 mmol/kg Cs-loaded vermiculite) and OS (783 mmol/kg Cs-loaded montomorillonite) complexes (fit data, dotted lines; experimental data, solids lines). The fitting results are summarized in Table 4.

TABLE 4. Fractions of IS and OS Cs Determined by Linear Combination Fitting Shown in Figure 4

sample	coverage (mmol/kg)	fraction IS[a] %	fraction OS[b] %
Cs on montmorillonite	783	0	100
Cs on montmorillonite	627	38	62
Cs on montmorillonite	538	48	52
Cs on vermiculite	271	52	48
Cs on vermiculite	190	65	35
Cs on vermiculite	159	100	0

[a] 100% IS is defined as the 159 mmol/kg Cs-loaded vermiculite sample. [b] 100% OS is defined as the 783 mmol/kg Cs-loaded montomorillonite sample.

in Cs coverage from 271 to 159 mmol/kg was accompanied by a decrease from 47% to 0% OS Cs (Table 4). We stress that the magnitude of these changes is only approximate due to the lack of proper reference spectra; using pure spectral components would improve accuracy. Nevertheless, the observed trends of decreasing OS sorption with Na^+ exchange are independent of the choice of reference spectra and substantiate the presence of two (or more) Cs sites on both vermiculite and montmorillonite at room temperature.

The environmental risks associated with the transport of Cs in the subsurface are largely a function of its coordination environment. Two distinct Cs coordination environments could be distinguished from our analysis of EXAFS structural parameters and linear combinations of spectra: (1) outer-sphere complexes and (2) one or more inner-sphere complexes in the ditrigonal cavity or at frayed edge sites. Cesium sorbed into OS complexes is easily exchangeable with Na^+ and, thus, is mobile in the environment, while IS sorption complexes may cause partial collapse of the interlayer, effectively limiting Cs mobility and bioavailability. These IS complexes are probably the dominant ones at low concentrations typical of radioactive Cs contamination; consequently, much of Cs in contaminated environments is expected to be strongly adsorbed. ^{133}Cs NMR (*4*, *5*) has been used to identify similar complexes at low temperature; however, thermal averaging causes the two spectral features to coalesce at room temperature. EXAFS can resolve these features at higher temperatures due to the faster timescale of its measurement. While further research is required to fully determine the structure of these disordered Cs sorption complexes, these data indicate the value of EXAFS in analyzing Cs coordination in natural matrixes.

Acknowledgments

This manuscript is based on research sponsored by the U.S. Department of Energy, Environmental Management Science Program under the prime Contract Nos. DE-AC02-98CH10886 and DE-FG07-99ER15012. The contribution from Brookhaven National Laboratory was supported in part by the U.S. Department of Energy NABIR program of the Office of Biological and Environmental Research.

Literature Cited

(1) Stevens, J. A. Sorption kinetics of Cs and Sr in sediments of a Savannah River Site Reservoir. M.S. Thesis, Colorado State University, Fort Collins, CO, 1996.
(2) McKinley, J. P.; Zeissler, C. J.; Zachara, J. M.; Serne, R. J.; Lindstrom, R. M.; Schaef, H. T.; Orr, R. D. *Environ. Sci. Technol.* **2001**, *35*, 3433−3441.
(3) Zachara, J. M.; Smith, S. C.; Liu, C.; McKinley, J. P.; Serne, R. J.; Gassman, P. L. *Geochim. Cosmochim. Acta* **2002**, *66*, 193−211.
(4) Kim, Y.; Cygan, R. T.; Kirkpatrick, R. J. *Geochim. Cosmochim. Acta* **1996**, *60*, 1041−1052.
(5) Kim, Y.; Kirkpatrick, R. J. *Geochim. Cosmochim. Acta* **1997**, *61*, 5199−5208.
(6) Chorover, J.; DiChiaro, M. J.; Chadwick, O. A. *Soil Sci. Soc. Am. J.* **1999**, *63*, 169−177.
(7) Cornell, R. M. *J. Radioanal. Nucl. Chem* **1993**, *171*, 483−500.
(8) Ohnuki, T.; Kozai, N. *Radiochim. Acta* **1994**, *66*−*7*, 327−331.
(9) Poinssot, C.; Baeyens, B.; Bradbury, M. H. *Geochim. Cosmochim. Acta* **1999**, *63*, 3217−3227.
(10) Brouwer, E.; Baeyens, B.; Maes, A.; Cremers, A. *J. Phys. Chem.* **1983**, *87*, 1213−1219.
(11) Kim, Y.; Kirkpatrick, R. J.; Cygan, R. T. *Geochim. Cosmochim. Acta* **1996**, *60*, 4059−4074.
(12) Weiss, C. A., Jr.; Kirkpatrick, R. J.; Altaner, S. P. *Geochim. Cosmochim. Acta* **1990**, *54*, 1655−1669.
(13) Serne, R. J.; Zachara, J. M.; Burke, D. S. *Chemical information on tank supernatants, Cs adsorption from tank liquids onto Hanford sediments, and field observations of Cs migration from past tank leaks*; PNNL-11495; Pacific Northwest National Laboratory: Richland, WA, 1998.
(14) Bjornstad, B. N. *Geohydrology of the 218-W-5 Burial Ground, 200 West Area, Hanford Site*; PNL-7336; Pacific Northwest Laboratory: Richland, WA, 1990.
(15) Kirkpatrick, R. J.; Yu, P.; Hou, X. Q.; Kim, Y. *Am. Mineral.* **1999**, *84*, 1186−1190.
(16) Staunton, S.; Roubaud, M. *Clays Clay Miner.* **1997**, *45*, 251−260.
(17) O'day, P. A.; Brown, G. E.; Parks, G. A. *J. Colloid Interface Sci.* **1994**, *165*, 269−289.
(18) O'day, P. A.; Parks, G. A.; Brown, G. E. *Clays Clay Miner.* **1994**, *42*, 337−355.
(19) Axe, L.; Bunker, G. B.; Anderson, P. R.; Tyson, T. A. *J. Colloid Interface Sci.* **1998**, *199*, 44−52.
(20) Peterson, M. L.; Brown, G. E.; Parks, G. A.; Stein, C. L. *Geochim. Cosmochim. Acta* **1997**, *61*, 3399−3412.
(21) Peterson, M. L.; Brown, G. E.; Parks, G. A. *J. Phys. IV* **1997**, *7*, 781−783.
(22) Bidoglio, G.; Gibson, P. N.; Ogorman, M.; Roberts, K. J. *Geochim. Cosmochim. Acta* **1993**, *57*, 2389−2394.
(23) Fendorf, S. E.; Lamble, G. M.; Stapleton, M. G.; Kelley, M. J.; Sparks, D. L. *Environ. Sci. Technol.* **1994**, *28*, 284−289.
(24) Fendorf, S. E.; Sparks, D. L. *Environ. Sci. Technol.* **1994**, *28*, 290−297.
(25) Kemner, K. M.; Hunter, D. B.; Bertsch, P. M.; Kirkland, J. P.; Elam, W. T. *J. Phys. IV* **1997**, *7*, 777−779.
(26) Kemner, K. M.; Hunter, D. B.; Elam, W. T.; Bertsch, P. M. *J. Phys. Chem.* **1996**, *100*, 11698−11703.
(27) Antonio, M. R.; Dietz, M. L.; Jensen, M. P.; Soderholm, L.; Horwitz, E. P. *Inorg. Chim. Acta* **1997**, *255*, 13−20.
(28) Sposito, G.; Le Vesque, C. S. *Soil Sci. Soc. Am. J.* **1985**, *49*, 1153−1159.

(29) Anderson, S. J.; Sposito, G. *Soil Sci. Soc. Am. J.* **1991**, *55*, 1569−1576.
(30) Smyth, J. R.; Spaid, A. T.; Bish, D. L. *Am. Mineral.* **1990**, *75*, 522−528.
(31) Ressler, T. *J. Phys. IV* **1997**, *7*, 269−270.
(32) Deleon, J. M.; Rehr, J. J.; Zabinsky, S. I.; Albers, R. C. *Phys. Rev. B* **1991**, *44*, 4146−4156.
(33) Zabinsky, S. I.; Rehr, J. J.; Ankudinov, A.; Albers, R. C.; Eller, M. J. *Phys. Rev. B* **1995**, *52*, 2995−3009.
(34) Sawhney, B. L. *Clays Clay Miner.* **1970**, *18*, 47−52.
(35) Berend, I.; Cases, J. M.; Francois, M.; Uriot, J. P.; Michot, L.; Masion, A.; Thomas, F. *Clays Clay Miner.* **1995**, *43*, 324−336.
(36) Comans, R. N. J.; Haller, M.; Depreter, P. *Geochim. Cosmochim. Acta* **1991**, *55*, 433−440.
(37) Comans, R. N. J.; Haller, M.; Vanderweijden, C. H.; Das, H. A. *Chem. Geol.* **1988**, *70*, 195−195.
(38) Smith, D. E. *Langmuir* **1998**, *14*, 5959−5967.
(39) Richardson, S. M.; Richardson, J. W. *Am. Mineral.* **1982**, *67*, 69−75.

Received for review September 9, 2001. Revised manuscript received March 25, 2002. Accepted April 1, 2002.

ES0156892